Journal of Thermal Analysis, Vol. 46 (1996) 1487-1500

THERMAL DEHYDRATION AND DECOMPOSITION OF $FeCl_3 \cdot xH_2O$

S. B. Kanungo and S. K. Mishra*

Regional Research Laboratory, Bhubaneswar–751013, Orissa, India

Abstract

Thermal dehydration and decomposition characteristics of Fe(III) chloride hydrate have been studied by both isothermal and non-isothermal methods. After the initial melting at 35–40°C both dehydration and decomposition of the salt proceed simultaneously at temperature above 100°C. At 250–300°C a stable hydrated $Fe(OH)_2Cl$ is formed representing the first plateau region in the TG curve. Around 400°C, a second plateau is observed corresponding to the formation of mostly Fe_2O_3 which however retains some OH groups and Cl^- ions. However, these temperature ranges vary with the TA equipments used. Chemical analysis of the products of decomposition at temperatures above 140°C also gives evidence for the formation of FeOCl which on hydrolysis in water gives $FeCl_3$ in solution. The FT–IR spectra suggest the presence of structural OH groups even for samples calcined at 300–400°C. The XRD patterns of the products of decomposition in the temperature range 160–400°C indicate the presence of β-FeOOH, some unidentified basic chlorides and α-Fe_2O_3.

Keywords: decomposition, dehydration, Fe(III) chloride hydrate

Introduction

The study of the thermal decomposition of hydrated Fe(III) chloride is of considerable importance in the field of extractive metallurgy. During the leaching of some base metal ores with high iron content, in HCl solution, or during chloridizing roasting of such ores by gaseous HCl, considerable amount of $FeCl_3$ is produced. Large quantities of both Fe(II) and Fe(III) chloride are also generated during the pickling of steel in conc. HCl. The aqueous solution of the salt is concentrated and pyrohydrolyzed to regenerate HCl and insoluble oxides of iron without affecting other valuable metal chlorides [1–7]. Extensive literature survey did not provide us with any worthwhile information on the thermal decomposition characteristics of $FeCl_3$ hydrate. This is because of the highly hygroscopic nature of $FeCl_3$ which makes it difficult to obtain this salt with a

* Author to whom all correspondence should be addressed.

0368–4466/96/ $ 5.00

John Wiley & Sons, Limited
Chichester

definite water of hydration and consequently reproducible thermal decomposition data. Despite this limitation an attempt has been made in this paper to study the dehydration and decomposition behaviors of $FeCl_3$ hydrate using both isothermal and non-isothermal methods. The products obtained after heating at different temperatures have been characterized by both physical and chemical methods.

Experimental

Materials

Analytical reagent grade $FeCl_3$ from Loba-Chemie (India) was used in the present work. Though the freshly opened bottle contained about 6 moles of H_2O per mole of $FeCl_3$, the value changed not only on storage but also during handling. Therefore, for each set of experimental run, a blank analysis of the sample was carried out to determine the water content. This value varied from 7.0 to 9.0 depending upon the relative humidity in the surrounding atmosphere.

Methods

Isothermal method

Isothermal mass loss experiments were carried out in a tube furnace of 25 mm internal diameter and maintained at ±4°C in the temperature range 100–250°C. About 200 mg weighed sample was taken in a series of glass boats of 7 cm in length. The furnace was first heated to the requisite temperature and when reasonable stability in temperature was attained one boat at a time was introduced into the maximum heating zone (ca. 15 cm) of the furnace. The boat was in contact with the tip of the Cr–Al thermocouple attached to the temperature control system. However, the temperature at the bottom of the boat was separately and continuously measured with a digital thermometer fitted with gas-filled sensor. The zero time was reckoned from the moment the sample was introduced into the furnace. After a specified period of heating, the boat was withrawn, cooled in a desiccator and weighed. Being aware that the method was relatively 'crude' the experiments were carried in duplicate and some in triplicate. Surprisingly, the maximum error was within ±4%. Because of this it was possible to construct mass loss curves even at an interval of 10°C.

Non-isothermal method

Non-isothermal dehydration and decomposition were carried out in a NETZSCH (model STA-409) as well as in a SHIMADZU (model DT-40)

equipments.* While cylindrical Pt crucible of 100 mg capacity was used in the former equipment to accommodate varying sample size, both alumina and platinum microcrucibles of maximum capacity 20 mg were used in DT-40. Both the equipments were calibrated using several known standard substances. It was observed that substances which show phase transitions exhibit closely similar peak temperatures (±3°C). However, substances releasing gaseous vapours during decomposition exhibit higher temperature (about 10–12°C) in STA-409. Various parameters such as heating rate, sample size and inert gas flow were studied to examine their effects on the thermograms of $FeCl_3$ hydrate using α-Al_2O_3 as a reference material.

X-ray diffraction

X-ray diffraction patterns of the products of decomposition were taken in a Phillips Diffractometer using CuK_α radiation with Ni-filter.

Infrared spectra

FT-IR spectra of the products of decomposition were taken in a BOMEM-100 (Canada) FT–IR Spectrophotometer using CsBr pellet technique. About 100 mg of CsBr dried at 500°C for 2 h was mixed uniformly with 1 mg of sample and pelletized under vacuum with 8–10 tonne pressure.

Chemical analysis

Two batches of the products of decomposition obtained after calcination for 1 h at different temperatures were used for chemical analysis. For one batch the entire product was dissolved in 25–30 ml of 4N HNO_3 at 70–80°C and the total volume was made up to 100 ml. For the other batch the product of calcination was leached at 60–70°C for 30 min in 25–30 ml of water, slightly acidified (*pH* 2.0–2.5) with one or two drops of 4N HNO_3. The insoluble portion was separated by filtration through G4 crucible. The residue after washing and drying at 120°C for 4 h was weighed and subsequently dissolved in hot 1:1 HNO_3 and the total volume was made up to 100 ml. Both filtrate and dissolved residue were analyzed for Fe and Cl contents according to the following methods.

Iron was estimated in a suitable aliquot by titrating with 0.01 *M* EDTA solution at *pH* 3.0 using sulphosalicylic acid as indicator. Chloride was determined by the Mohr's titration with 0.01 *M* $AgNO_3$ using K_2:CrO_4 as indicator.

---

* It was not the objective of this paper to judge the suitablility of one equipment over the other,but to show how the thermal curve of a sample might vary with the equipment used.

Results and discussion

Isothermal dehydration and decomposition

As Fe(III) chloride hydrate decomposes almost completely in the temperature range 100–200°C isothermal experiments were carried out at short intervals of 10–20°C. Figure 1 depicts the variation in total mass loss with respect to time and temperature. The loss increases almost uniformly with increase in temperature from 105 to 125°C mainly due to dehydration of the molten salt, but shows sharp increase beyond this temperature due to the onset of rapid dehydrochlorination reaction. At 195°C a maximum (total) loss of 60.5% is observed in about 20 min of heating, against the calculated loss of about 59.7% for the possible formation of $Fe(OH)_2Cl$ from $FeCl_2 \cdot 8H_2O$.

In order to obtain more information about the extents of both dehydration and dehydrochlorination, the products obtained after 1 h of heating at different temperatures were analysed for Fe, Cl and H_2O contents. Other physical methods, such as XRD and FT–IR spectroscopy were used to characterize the products.

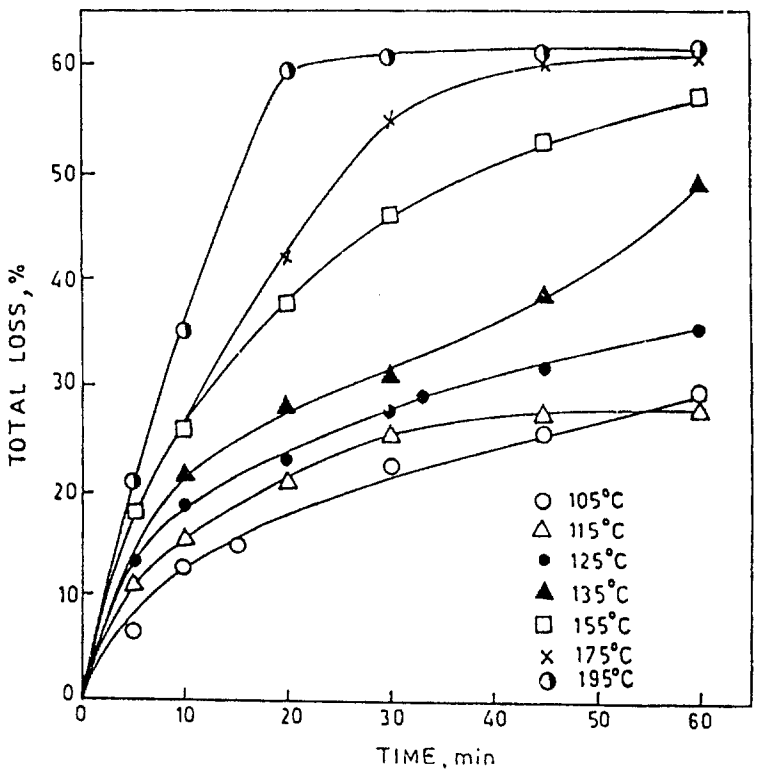

Fig. 1 Isothermal mass loss (total) as a function of time for the dehydration and decomposition of Fe(III) chloride hydrate at different temperatures

Table 1 Chemical analysis of the products of decomposition of Fe(III) chloride hydrate at different temperatures for 1 h

T/ °C	Total weight loss/ %	Total Fe/ %	Total Cl/ %	Moles of H_2O present in the product	Cl:Fe mol ratio in the product
105	28.8	26.94	50.74	2.57	2.97:1
115	28.5	27.69	50.09	2.49	2.85:1
125	35.4	30.27	45.71	2.46	2.38:1
135	50.2	41.77	40.00	1.02	1.51:1
155	56.9	45.41	37.32	1.18	1.29:1
175	60.6	49.90	34.81	0.96	1.10:1
200	61.2	50.00	32.27	1.10	1.02:1
300	61.6	51.00	30.06	1.15	0.93:1
400	75.2	62.42	2.00	0.96	0.05:1

Chemical analysis

Table 1 shows the results of chemical analysis along with mass loss data after 1 h of calcination of $FeCl_3 \cdot 8H_2O$. It can be seen that total mass losses at 105 and 115°C are almost same, although chemical analysis indicates higher losses of H_2O and Cl. This indicates that the initial states of hydration of the salt were little different for this two temperatures. Such variation takes place during sample preparation and handling before calcination and is, of course, within the limits of experimental error. The mass loss registers a sharp increase from 125 to 175°C at which Cl:Fe mole ratio is close to unity. However, the interesting aspect of the data in Table 1 is that the mole of OH or oxygen in the product remain almost constant at unity from 135 to 200°C, although Cl/Fe ratio decreases gradually from 1.5 to 1.0. Since no information is available from literature on the formation of any hydrolysed species of $FeCl_3$ and the assumed compound $Fe(OH)_2Cl$ contains 2 moles of OH (equivalent of 2 moles of H_2O), the product at 200°C is therefore FeOCl along with some adsorbed moisture which gives rise to O–H stretching band in the IR spectrum (see infra). The loss of chlorine in the intervening temperature range takes place from the intermediate mixture of $FeOCl \cdot H_2O$ and $Fe(OH)Cl_2$.

The total analysis of the decomposition products as shown in Table 1 does not provide sufficient information on the phases present in them. Therefore, the products of decomposition were separated into 'soluble' and 'insoluble' fractions by careful leaching in slightly acidified water. Table 2 shows the quantities of two fractions and their compositions. The results show that the maximum extent of decomposition is attained even at 140°C. It is interesting to note that the

Table 2 Chemical analysis of water soluble and insoluble fractions of the products of decomposition of Fe(III) chloride hydrate at different temperatures for 1 h

T/ °C	Total weight loss/ %	Insoluble fraction (x_i)/ %	Cl:Fe mol ratio in x_i	Soluble fraction (x_s) %	Cl:Fe mol ratio in x_s
100	28.1	6.2	0.47:1	93.8	3.08:1
120	40.6	19.6	0.31:1	80.4	3.05:1
140	59.8	93.3	0.43:1	6.7	3.11:1
160	60.8	89.7	0.40:1	10.3	3.13:1
180	60.9	86.5	0.52:1	13.5	2.61:1
200	60.9	91.3	0.57:1	8.7	3.20:1

quantity of insoluble fraction does not show any large change from 140 to 200°C. This is possibly due to the hydrolysis of a portion of $FeCl_3$ in water to yield $FeCl_3$ [8]. As a result, a certain quantity of soluble $FeCl_3$ is always obtained even for the product obtained at 200°C of calcination.

$$3FeOCl\ (s)+H_2O\ (l)\rightarrow FeCl_3+2FeOOH\ (s)$$

The little variation in the quantity of insoluble fraction in the temperature range 140–200°C is due to the variation in the extent of hydrolysis affected by factors such as *pH*, temperature etc. The insoluble fraction is therefore a mixture of FeOOH and $FeOCl{\cdot}H_2O$ showing a Cl:Fe ratio close to 0.5.

X-ray diffraction

Figure 2 illustrates the XRD patterns of the products of decomposition at different temperatures. The figure shows that no definite product is crystallized out form the molten phase up to 140°C. At temperature around 160°C crystalline product begins to appear, although no definite phase can be identified. The JCPDS powder files give patterns for only two chlorine-bearing oxyhydroxide of iron, namely β-FeOOH (akaganeite) and $xFe(OH)_2$, $FeOCl{\cdot}2H_2O$ besides FeOCl, but no pattern of the compound $Fe(OH)_2Cl$ is available. The diffraction patterns of the product obtained at 160 and 200°C suggest the presence of β-FeOOH, some form of complex oxychlorides and α-Fe_2O_3. At 400°C the product is identified mainly as α-Fe_2O_3.

Infrared spectra

Both chemical analysis and XRD pattern suggest the presence of free as well as structural OH groups in the calcined product of Fe(III) chloride hydrate. It is

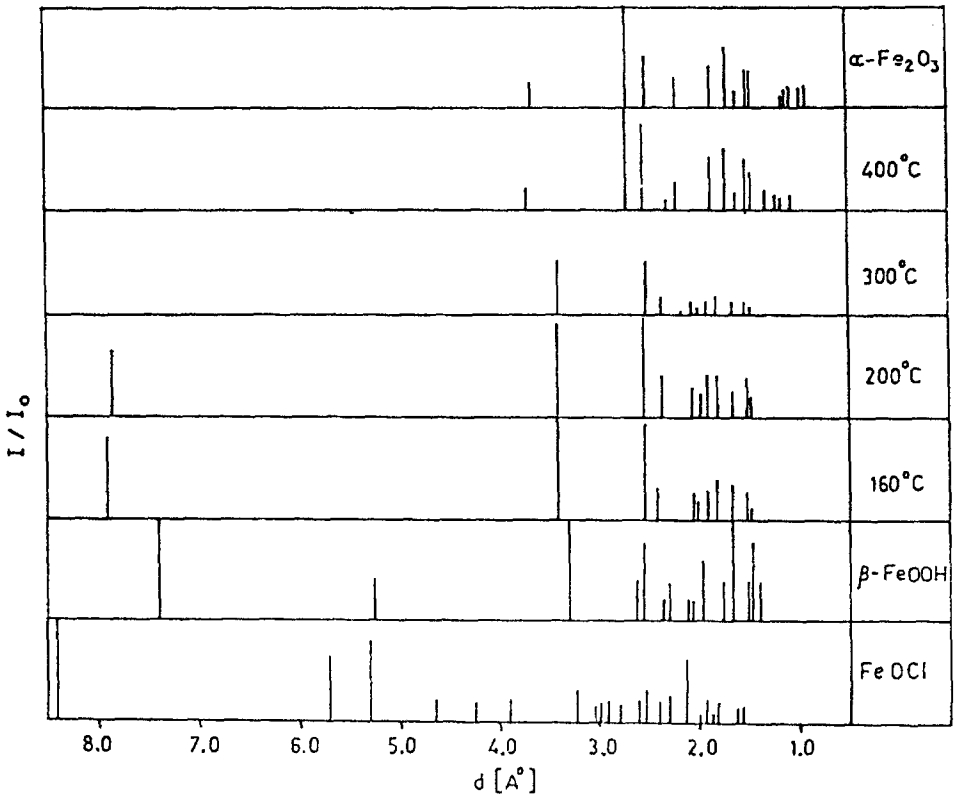

Fig. 2 X-ray diffraction (XRD) pattern of the products of the decomposition of Fe(III) chloride hydrate at different temperatures

well-known that free water shows broad absorption band in the region around 3400 cm^{-1} (stretching) and a sharp band around 1630 cm^{-1} (bending mode). However, unlike those from dispersive type spectrophotometer, FT–IR spectra (Fig. 3) shows a number of bands in the region of 3200–3500 cm^{-1} for the sample calcined at 120–235°C. The shift in the fundamental O–H frequency from around 3600 cm^{-1} to 3200–3500 cm^{-1} and the multiplicity of the bands in this region indicates that there are more than one type of hydrogen bounded OH groups (e.g. O–H...O and O...H–Cl). The intensity of the bending mode of free water gradually decreases and is almost absent in the sample calcined at 235°C. The major changes in the spectra (Fig. 3) with increase in calcination temperature are: (1) Gradual decrease in the number of bands due to hydrogen bonded OH groups in the region 3200–3500 cm^{-1}. It is worthwhile to note that such OH groups are not fully eliminated even for the sample calcined at 435°C. (2) Reshifting of OH stretching bands to frequencies higher than 3500 cm^{-1} clearly

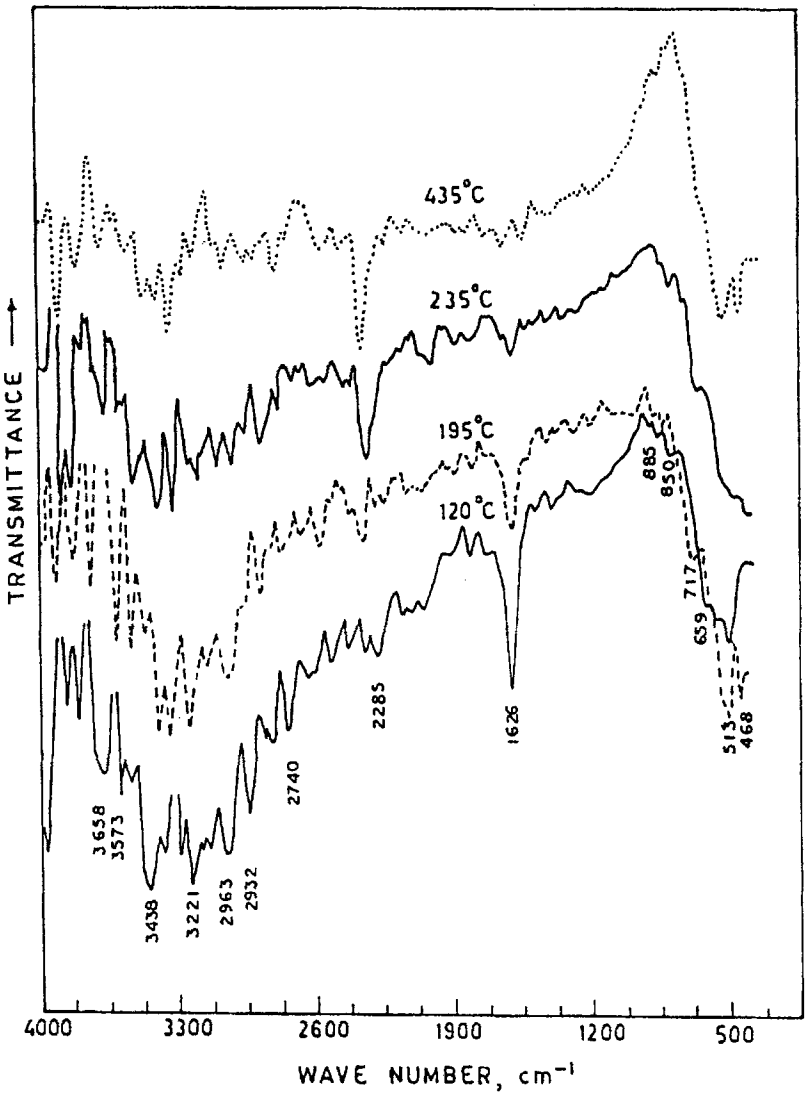

Fig. 3 FT-IR spectra of the products of the decomposition of Fe(III) chloride hydrate at different temperatures

suggest the breaking up of hydrogen bonded OH groups. (3) Increase in the intensity of the band around 2365 cm^{-1} which is attributed to MOH stretching vibration. (4) Complete disappearance of the bending mode due to Cl–Fe–OH vibration at 435°C in the region 850–640 cm^{-1}. (5) Appearance of characteristic Fe–O vibration for the unit cell of Fe_2O_3 in the frequency region 550–450 cm^{-1}.

Non-isothermal method

Effect of heating rate

This parameter was studied by using both STA-409 and DT-40 models. Let us first examine the TA curves obtained from STA-409 under static air environment using about 50 mg of sample (Figure not shown due to space constraint). At 2°C min^{-1} the resolution of DTA peak is rather poor, but becomes sharper with increase in heating rate. Apart from initial melting which takes place at low temperature (35–40°C) two broad endothermic effects can be observed in the temperature range 60–250°C. The first in the range 120–180°C represents the loss of about 4 moles of water which is immediately followed by the loss of remaining water simultaneously with the loss of HCl. Therefore, the second endo effect at 200–255°C appears to be the overlapping of both dehydration and dehydrochlorination reactions. The appearance of a small but sharp spike at the end of the otherwise very broad endothermic effect, possibly represents a change of phase due to the formation of decomposition product according to the following reactions.

$$FeCl_3 \cdot xH_2O\ (s) \longrightarrow FeCl_3 \cdot 2H_2O\ (s) + (x-2)H_2O\ (g)$$

$$FeCl_3 \cdot 2H_2O\ (s) \longrightarrow FeOCl \cdot H_2O\ (s) + 2HCl\ (g)$$

$$FeOCl \cdot H_2O\ (s) \rightleftharpoons FeOCl\ (s) + H_2O\ (g)$$

The hydrated ferroxy chloride is formed due to the adsorption of water vapour from the ambient atmosphere by FeOCl [8]. The observed mass loss in the first plateau region of TG curve is about 60.5% which corresponds to the formation of $FeOCl \cdot H_2O$. Therefore, anhydrous ferroxy chloride is not formed under dynamic condition because of the presence of H_2O vapour in the ambient atmosphere, unlike heating for a longer period (at least 1 h) under isothermal condition. Indeed, FeOCl is reported to be formed by the decomposition of anhydrous $FeCl_3$ in air [9].

Considering that the first plateau region corresponds to the formation of $FeOCl \cdot H_2O$, the number of moles of H_2O presents initially in the sample can be obtained from the following relationship.

$$\alpha = (18x + 37)/(162.35 + 18x)$$

where α = fraction of weight loss at the first plateau region, x = number of moles of H_2O present in the initial stage.

The values of x given in Tables 3 and 4 indicate that there is a considerable variation in the initial water content of the salt due to its highly hygroscopic character which is difficult to avoid during handling.

Table 3 Non-isothermal dehydration and decomposition data of Fe(III) chloride hydrate ($FeCl_3 \cdot xH_2O$) obtained from NETZSCH STA-409 under different experimental conditions

Heating rate or sample size	Melting point °C	First stage of dehydration			Second stage of dehydration and decomposition				Third stage of decomposition	
		T_i-T_c/ °C	$T_{DTA\ peak}$/ °C	Moles of water lost	T_i-T_c/ °C	$T_{DTA\ peak}$/ °C	$\Delta m_1^{a)}$/%	x in $FeCl_3 \cdot xH_2O$	$\Delta m_2^{b)}$/%	Calcd. loss[c]
A. Effect of heating rate °C min^{-1}; Sample size: 50 mg										
2	30	–	90	5.1	120–190	185	60.5	8.6	–	–
5	35	60–160	120	4.7	170–215	205	60.4	8.5	71.9	74.7
10	40	70–190	150	4.1	200–260	230	57.2	7.3	67.6	72.7
20	40	85–205	180	4.0	205–320	255	59.8	8.3	71.0	74.4
B. Effect of sample size, mg; Heating rate: 10°C min^{-1}										
15.80	40	60–150	120	4.9	190–230	210	60.7	8.7	72.8	75.0
30.90	40	60–170	110	4.0	180–240	210	58.3	7.7	69.9	73.5
52.80	40	70–190	150	4.1	200–260	230	57.2	7.3	67.6	72.7
76.80	45	80–200	180	5.3	220–290	260	63.5	10.0	74.9	76.6
51.47**	40	60–170	145	4.4	190–300	260	61.6	9.1	72.5	75.5

* T_i =temperature of inception, T_c =temperature of completion

** Flowing nitrogen environment (50 ml min^{-1})

a) Δm_1 = mass loss at the first plateau in TG curve

b) Δm_2 = mass loss at the second plateau in TG curve

c) calculated total loss on the basis of formation of Fe_2O_3 as the final insoluble product.

On further heating a second plateau region is observed in the TG curve at temperature around 400°C with a mass loss of about 71–73%. Unless a high heating rate is used no DTA peak can be distinguished for this stage which corresponds to the following possible reaction (mass loss 71.6%)

$$FeOCl{\cdot}H_2O\ (s) \rightarrow FeOOH\ (s) + HCl\ (g)$$

From the XRD patterns of the decomposition products no FeOCl has been identified. On the other hand, the presence of β-FeOOH in the product has been detected in the XRD pattern. It is well-known that β-FeOOH retain some Cl^{-1} in its framework structure [10]. Since at 400°C and above β-FeOOH is not stable [11, 12], the following sequence of overall reactions in proposed.

$$FeCl_3{\cdot}xH_2O\ (s) \xrightarrow{250°C} FeOCl{\cdot}H_2O\ (s) + (x-2)H_2O\ (g) + 2HCl\ (g)$$

$$FeOCl{\cdot}H_2O\ (s) \xrightarrow{300°C} FeOOH\ (s) + HCl\ (g)$$

$$FeOOH\ (s) \xrightarrow{400°C} 1/2Fe_2O_3\ (s) + 1/2H_2O\ (g)$$

adding

$$FeCl_3{\cdot}xH_2O\ (s) \longrightarrow \frac{(2x-3)}{2}H_2O\ (g) + 3HCl\ (g) + 1/2Fe_2O_3\ (s)$$

The above sequence of reactions corresponds to a total mass loss of 73.8%. The data in Table 3 shows that the calculated values are 2–3% higher than those found from TG curves. This is possibly due to the retention of some OH and Cl in the Fe_2O_3 structure obtained from the calcination of β-FeOOH.

The above thermal effects are better resolved in the thermal curves obtained from Shimadzu DT-40 model, using about 15 mg sample in an alumina crucible (Fig. 4). Except for the initial melting, the other two thermal effects appear at temperatures 20–40°C lower than those from STA-409. The endothermic effect due to first major water loss appears as a broad but distinct peak. However, the nature of the second endo peak due to dehydration and decomposition is almost similar to that appeared in STA-409. The amount of water lost in the first stage of dehydration is generally about 4 moles as also found in STA-409. However, when the thermoanalytical curves are taken in DT-40 using Pt crucible, the second stage of dehydration and decomposition is resolved into two distinct endothermic effects (figure not shown). It may be noticed that except for the initial melting, the DTA peak temperatures for other reactions are little higher than those obtained by using alumina crucible. The results are summarized in Table 4.

Table 4 Non-isothermal dehydration and decomposition data of $FeCl_3 \cdot xH_2O$ obtained from Shimadzu, DT-40 under different rates of heating using alumina and platinum crucibles

Heating rate/ °C min^{-1}	Melting point/ °C	First stage of dehydration			Second stage of dehydration and decomposition			
		T_i–T_c*/°C	$T_{DTA\ peak}$/°C	Moles of water lost	T_i–T_c*/°C	$T_{DTA\ peak}$/°C	Δm_1[c]	x in $FeCl_3 \cdot xH_2O$
A. Results obtained using alumina crucibles; sample size: 15–17 mg								
2	37.0	–	63.7	–	–	–	–	–
5	35.8	42–120	75.0	3.4	132–164.5	160.0	51.0	5.0
8	37.5	43–112	82.5	3.5	126–187	165.0	56.4	2.0
10	37.5	42.5–112	80.5	4.0	126–190	163.5	60.0	8.4
15	37.5	45–150	88.0	4.1	150–220	177.5	55.0	6.5
20	39.0	47–152	93.0	4.9	152–230	175.0	61.5	9.0
B. Results obtained using platinum crucibles; sample size: 15 mg								
4	36.5	46–135	96.0	4.5	170–195	172.0[a] 180.0[b]	59.4	8.1
6	37.0	45–145	96.0	5.5	165–220	177.0[a] 185.0[b]	62.5	9.5
8	38.5	56–150	102.0	4.4	150–205	180.0[a] 190.0[b]	59.1	8.0
10	37.0	43–160	103.0	4.5	160–210	178.0[a] 190.0[b]	60.9	8.8
12	38.0	43–160	108.0	4.9	160–230	180.0[a] 198.0[b]	62.3	9.4

* Temperature range: T_i=temperature of inception, T_c=temperature of completion

a) Temperature for the first endothermic peak; b) temperature for the second endothermic peak; c) Δm_1=mass loss at the first plateau in TG curve.

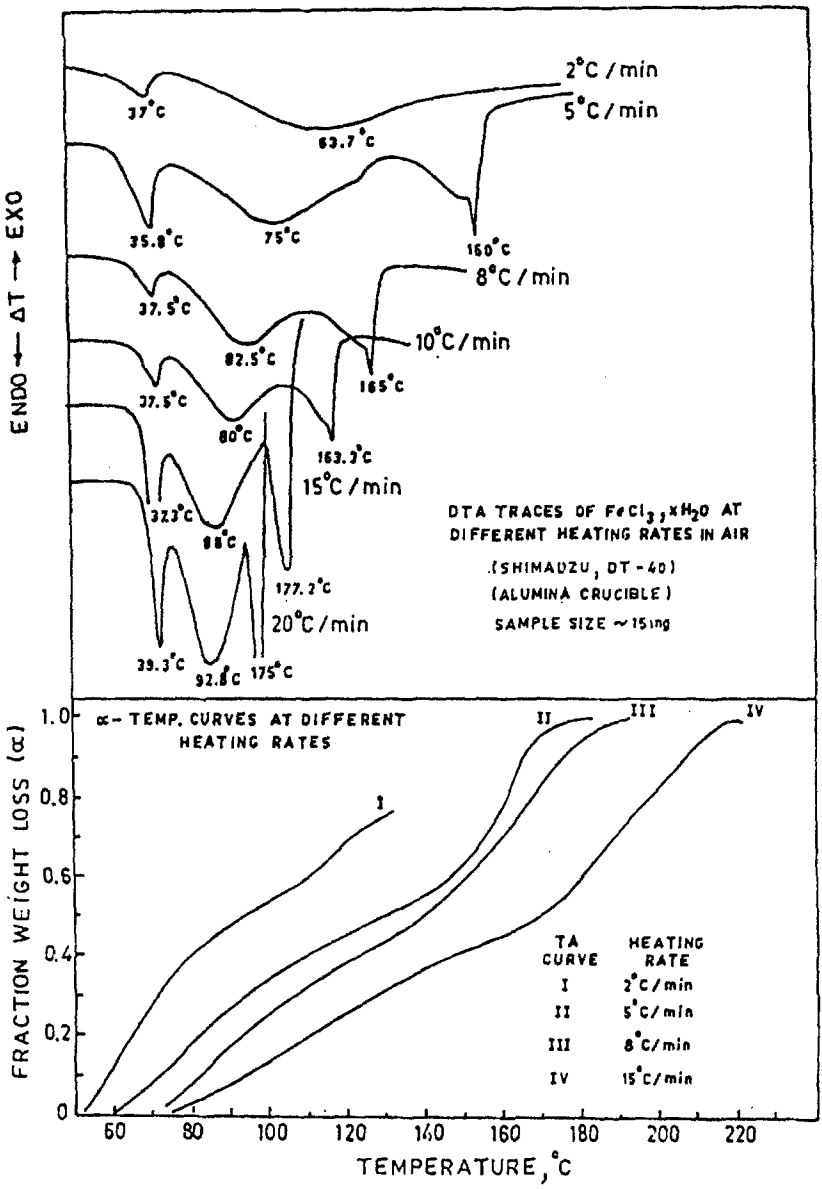

Fig. 4 Thermoanalytical curve of Fe(III) chloride hydrate obtained from SHIMADZU (DT-40) at different rates of heating using alumina crucible

ond stage of dehydration and decomposition is resolved into two distinct endothermic effects (figure not shown). It may be noticed that except for the initial melting, the DTA peak temperatures for other reactions are little higher than

those obtained by using alumina crucible. The results are summarized in Table 4.

Effects of sample size and inert gas flow

The nature of the TA curves of $FeCl_3$ hydrate does not change with increase in sample size from 15.8 to 76.8 mg except that the DTA peak temperatures tend to increase with increase in size (Table 3). Similarly, the nature of the TA curves in flowing nitrogen environment remains unaltered except that the final mass loss shows little higher value (Table 3).

The difference in DTA peak temperatures in the TA curves obtained from the two equipments is possibly due to the differences in designs of (a) detector vis–à–vis sample holder and (b) furnace and thermocouple assembly. While in STA-409 the hollow protruded bottoms of the crucibles rest on the thermocouple tips, in DT-40 the base of the cylindrical crucibles rest on circular Pt discs below which the thermocouple tips are fused. In STA-409 the furnace is of larger size (height 230 mm, dia 50 mm) than that of DT-40 (height 60 mm, dia 23 mm) with SiC and platinum resistance wire serving as heating elements respectively. Another notable difference in the two equipments is that while in STA-409, the entire thermocouple assembly is covered by an alumina jacket closed at the top, in DT-40 it is opened at the top. As a result, samples releasing gaseous vapours during heating tend to exhibit higher temperature in the former equipment compared to that in the latter.

* * *

The authors wish to thank the Director, R. R. L. Bhubaneswar for his kind permission to publish this paper. One of the authors (SKM) is grateful to the Council of Scientific and Industrial Research (CSIR), New Delhi for the award of a fellowship.

References

1 M. L. Skow, R. C. Kirby and J. E. Conley, Rept. Invest. U. S. Bur. Mines, No. 5171, p. 29.
2 U. Scheffer and K. H. Ulrich, Ger. Offen. 2, 249, 302 (to Friedrich Krupp, G.m.b.H).
3 K. N. Han and D. W. Fuerstenau, Miner. Processing Technol Rev., 1 (1983) 1.
4 P. B. Queneau and H. J. Roorda, Min. Eng., 23 (1971) 70.
5 H. Jedlicka, Proc. Symp. on chloride hydrometallurgy, Brussels 1977, p. 182.
6 H. N. Sinha and J. R. Tufley, Extractive metallurgy '81, The Inst. Mining Metallurgy, London 1981, p. 421.
7 A. Van Peteghem, U. S. Pat 4, 026, 773, May 3, 1977 (to Metallurgie Hoboken Oberpelt).
8 J. W. Mellor, Comprehensive Treatise on Inorganic and Theoretical Chemistry, Vol. 14, Longmans, London 1965, pp. 72–73.
9 A. W. Henderson, T. T. Campbell and F. E. Block, Metal. Trans., 3 (1972) 2579.
10 J. Ellis, R. Giovanoli, W. Sturm, Chimia, 30 (1976) 141.
11 T. Ishikawa and K. Inouye, Bull. Chem. Soc., (Japan) 48 (1975) 1580.
12 E. Peterson, R. Swaffield and D. R. Clark, Thermochim. Acta, 54 (1982) 201.